RESEARCH ON THE THERMAL AND FLOW CHARACTERISTICS OF NOVEL MICRO-CHANNEL PV/T COLLECTORS

by

Guoqing YU**, Wubin DING, and Cheng XU

School of Environment and Architecture,
University of Shanghai for Science and Technology, Shanghai, China

Original scientific paper
https://doi.org/10.2298/TSCI230522227Y

A novel micro-channel PV photothermal collector is investigated, comprising of PV cells and collectors. Its distinctive feature lies in the flow mode of its micro-channels. The novel micro-channel investigated in this study is composed of multiple drums, allowing for a non-parallel flow configuration. This distributional flow pattern facilitates enhanced contact between the water flow and the heat transfer surface, thereby resulting in significantly improved heat transfer efficiency. Characteristics and flow properties are studied to enhance the thermoelectric performance and broaden the application scope of PV photothermal collector technology. This study focuses on parallel micro-channels and three-passes micro-channels for comparison, employing ANSYS FLUENT to simulate electrical and thermal efficiencies, temperature distribution, velocity field, and pressure field under typical operating conditions. The validity of the model is verified by comparing it with experimental panel surface temperature data. Within this framework, various inlet flow conditions are examined to investigate the collector's temperature profile, standard deviation of temperature distribution, pressure drops, and maximum velocity. Results indicate that under specific circumstances, the heat collection performance of parallel micro-channel PV photothermal collectors is inferior to that of three-passes micro-channel counterparts. Both types exhibit reduced efficiency during winter conditions, however, three-passes micro-channels experience a more significant decline at 22.4%, compared to 19.7% for parallel micro-channels. In terms of flow resistance characteristics, parallel micro-channels demonstrate advantages in terms of pressure drops over three-passes configurations as they exhibit nearly 3935 Pa lower values under certain conditions. Regarding temperature uniformity in PV-photothermal systems, parallel micro-channel collectors outperform their three-passes counterparts.

Key words*: PV photothermal collector, micro-channel, electrical efficiency, pressure drops, thermal efficiency*

Introduction

PV/thermal (PV/T) technology was initially proposed by Wolf in 1976 [1]. The integration of solar PV and thermal systems enables the simultaneous generation of electricity and heat, thereby significantly enhancing the utilization efficiency of solar energy.

*Corresponding author, e-mail: yuguoqinghvac@126.com

Currently, the primary focus of PV/T collector research lies in enhancing its thermoelectric efficiency. Many scholars have conducted comprehensive reviews on the research and development of PV/T collectors from various perspectives. Balji *et al.* [2] categorized PV/T collectors into air-based and water-based systems, and conducted a comparative analysis between PV/T collectors and conventional PV systems. Yang and Athienitis [3] provided a comprehensive overview of the research and development progress in PV/T collector technology until 2016, categorizing them into air systems, water systems, and phase change material systems. Debbarma *et al.* [4] conducted a comprehensive analysis of PV systems in comparison with PV/T collectors, encompassing mathematical models, numerical simulations, and system performance evaluations. Shukla *et al.* [5] conducted a comprehensive investigation into the developmental trajectory and evolving electrical performance of building integrated PV systems.

Initially, Wei *et al.* [6] conducted experiments to compare the photo-thermal and photoelectric performance of water-cooled PV/T collectors with traditional solar water heaters and PV modules. The results showed that when the initial water temperature in the system was the same as the daily average ambient temperature, the daily thermal efficiency could reach about 40%, and the photo-thermal integration was significantly higher. Yandri [7] reshaped the thermal efficiency model of the hybrid PV/T collector during the steady state to develop the operation mode factor. Joule heat occurs when the PV panel operates at a high current during the maximum power point tracking at higher irradiation. Under these conditions, some electrical energy is converted into heat energy in the PV battery. Joule heating helps to improve PV/T thermal efficiency. Zhou *et al.* [8] investigated a novel solar driven direct-expansion heat pump system employing micro-channel PV/T modules as the evaporator, and the overall efficiency is about 69%. Atazaz *et al.* [9] proposed the numerical and experimental checks of various parameters of the hybrid PV thermal system (PV/T) to improve the heat transfer performance of the PV thermal system. The effects of flow parameters, tube diameter and substrate thickness on the heat transfer, electrical and overall performance characteristics of water-based PV/T were investigated. The results show that when the Reynolds number increases, the PV thermal (PV/T) system increases. With increasing Reynolds number, the heat transfer rate of the PV/T system is likely to increase by the 15%. Tahmasbi *et al.* [10] used metal foam to improve the thermal efficiency and electrical efficiency of solar PV heat/air system (PV/T/air) which the thermal efficiency and electrical efficiency are increased by about 85% and 3% by porous foam. Satpute and Rajan [11] presented a novel thermal absorber based PV-T system. The thermal absorber is attached at the rear surface of PV, and water is recirculated to extract heat. The results revealed that the annual CO_2 mitigation for PV and PV-T system was 225.46 kg annual and 464.8 kg annual, while simple payback periods were 4.53 years 3.03 years, respectively.

However, limited research has been conducted on micro-channel PV/T collectors. The integration of the heat absorber within the micro-channel structure offers significant advantages for PV cells, including a larger heat transfer area, enhanced conversion efficiency, and reduced surface temperature. Moreover, the implementation of a micro-channel heat exchanger ensures rapid thermal response and excellent isothermal performance [12]. Hesham *et al.* [13] investigates the integration of the double-layer micro-channel radiator with the CPV battery as a thermal management device in order to enhance its heat dissipation capabilities under varying ground conditions.

Therefore, it is imperative to conduct a comprehensive investigation on high-efficiency micro-channel PV/T collectors in order to enhance their thermoelectric performance, address existing challenges, and broaden the application scope of PV/T technology. This study focuses on examining two variants of micro-channel PV/T collectors: parallel and three-passes configurations. The conventional micro-channel typically comprises numerous parallel flat tubes, collector tubes, baffles, and other components. Each flat tube contains multiple intricate channels. However, the novel micro-channel investigated in this study is composed of multiple drums, allowing for a non-parallel flow configuration. This distributional flow pattern facilitates enhanced contact between the water flow and the heat transfer surface, thereby resulting in significantly improved heat transfer efficiency. Simulations are conducted by using Ansys Fluent and validated against experimental data.

System description

Three-passes micro-channel PV/T

The configuration of the three-passes micro-channel PV/T system, as depicted in fig.1, consists of a PV cell, an absorbing plate, a micro-channel layer, and insulation. To fabricate the micro-channels, a stainless-steel plate is initially pressed to form bulges with identical diameters and spacing in a staggered arrangement. Subsequently, this plate is welded onto another piece of 304 stainless steel plate of the same size. The three-passes micro-channel PV/T device features a single inlet and outlet for fluid flow through three passes within the channel network, fig. 2. The overall dimensions of the PV/T collector are 1.2 meters in length, 0.6 meters in width, and 30 mm in thickness.

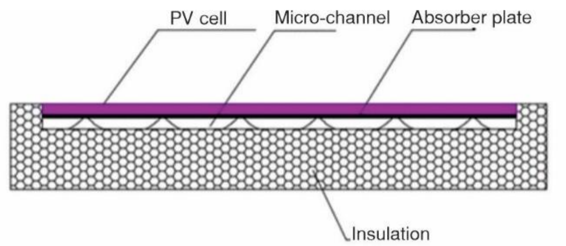

Figure 1. The structure of the unglazed micro-channel PV/T collector

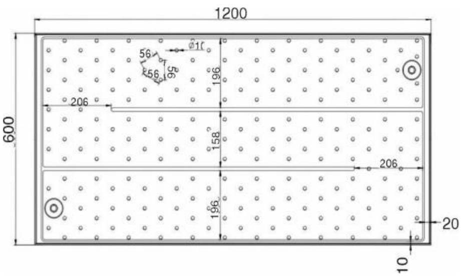

Figure 2. The surface of three-passes micro-channel PV/T collector

Parallel micro-channel PV/T

The configuration of the parallel micro-channel PV/T system is identical to the three-passes micro-channel PV/T system, fig. 3. It comprises a sequential arrangement from top to bottom: the PV (PV) cell, absorber plate, micro-channels, and insulation layer. The dimensions of the parallel micro-channels closely resemble those of the three-passes micro-channels; however, the parallel micro-channels possess three distinct flow channels with individual inlet and outlet ports as illustrated in fig. 4.

Before the simulation, the laboratory conducted rigorous testing on the experimental data using a range of sophisticated instruments, including the Honle artificial light source (VG-Kasten SOL 2000), EKO IV Curve tester (MP-170), East Star hot and cold dual-use thermostatic chiller (DX-01A), GRAPHTEC data collector (Midi LOGGER GL800), and Solar irradiator. These state-of-the-art equipment ensured accurate measurements and reliable results for our study.

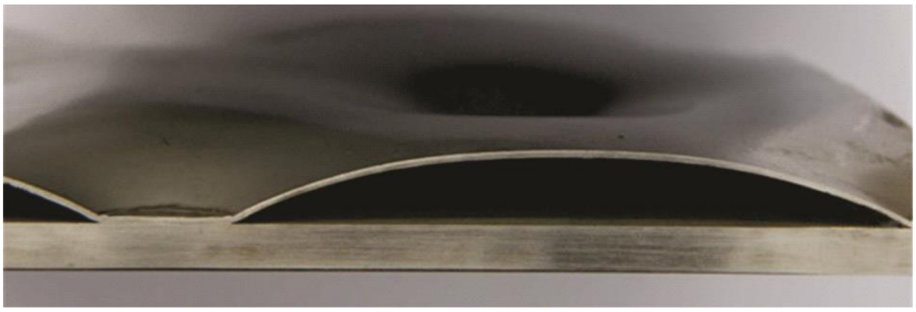

Figure 3. Local enlargement of the three-passes micro-channel plate

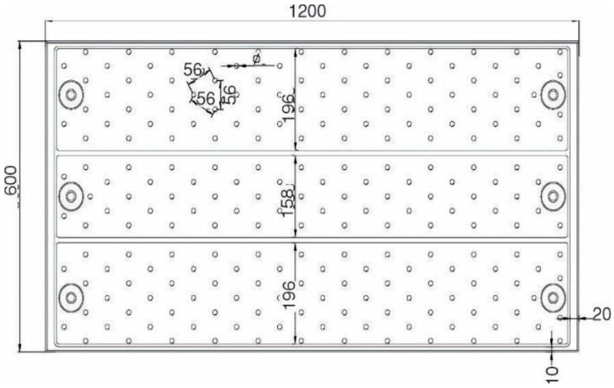

Figure 4. The surface of parallel micro-channel PV/T collector

Modeling description

The PV/T collector model construction and meshing

The PV/T collector model was successfully developed using the ICEM CFD software, a robust modeling and grid generation tool provided by ANSYS. This software offers grid files for numerical simulations in FLUENT and other applications. Notably, ANSYS ICEM CFD

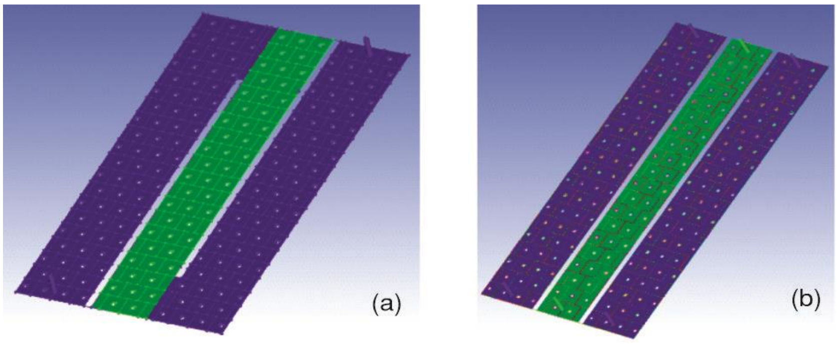

Figure 5. (a) The model of three-passes Micro-channel and (b) the model of parallel micro-channel PV/T

stands out as the most powerful hexahedral structured grid generation tool currently available on the market. As for the remaining components of the PV/T collector, including the PV cell, heat absorber plate, and insulation material. The micro-channel structure exhibits a relatively intricate configuration, where two parallel planes intersect with a sphere. Consequently, we have successfully constructed a PVT device featuring a corrugated plate as its key component. fig. 5(a) illustrates our three-passes micro-channel PV/T model.

The flow path of the parallel micro-channel closely resembles that of the three-passes micro-channel. The connection between the three corrugated plates has been eliminated, resulting in three separate corrugated plates. The model depicting the parallel micro-channel PV/T can be observed in fig. 5(b).

After drawing the model, it should be divided into various components including PV panels, heat absorption plates, water channels, insulation layers, fluid inlets, fluid outlets and surrounding walls. The simulation employs a structured grid for generating the mesh as depicted in fig. 6(a), with a partial zoom displayed in fig. 6(b). The mesh exhibits high quality with an average mass of 0.96.

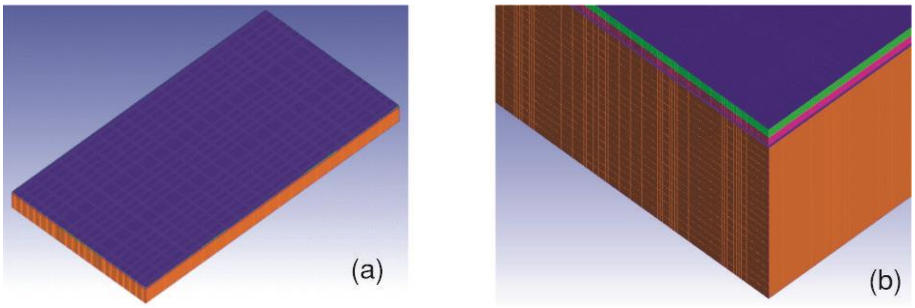

Figure 6. (a) The grid of the PV/T and (b) partial enlargement of the grid of PV/T

Fluent simulation parameter settings

To guarantee the precision of simulation outcomes and optimize computational efficiency, we have made the following assumptions:
- The simulated operating conditions are in a steady state, with the temperature and velocity of the inlet fluid as well as the ambient temperature being held constant.
- The radiative heat loss from the PV/T collector to the sky are not considered.
- The power generation performance of the PV/T cell is not considered, and only the heat collection performance of the PV/T collector is investigated, considering the PV/T cell as an internal heat source.
- The physical parameters of the material are constant.

Taking the parameter settings of the parallel micro-channel PV/T collector as an example, the case file parameters were configured in FLUENT after importing the mesh file. A pressure-based solver with steady state time was employed for solving. The computational model incorporates energy exchange throughout, necessitating activation of the energy equation. Turbulent fluid flow pattern in the micro-channel is simulated using the standard k-ε viscosity model. The materials utilized include glass, PV cells, stainless steel, copper, and insulation; their respective parameters are presented in tab. 1.

The SIMPLE model is employed for calculating the model, with the gradient model being Least Squares Cell Based, and the pressure model being PRESTO!. The relaxation factors

Table 1. Parameters of each material

Material	Density [kgm^{-3}]	Capacity [Jkg^{-1}°C^{-1}]	Thermal conductivity [Wm^{-1}°C^{-1}]	Viscosity [kgm^{-1}s^{-1}]
PV cell	1500	1760	10	–
Stainless steel	7930	500	16.3	–
Water	998.2	4182	0.6	0.001003
Insulation	50	800	0.1	–
Aluminum	2719	871	202.4	–

are set as: 0.3 for pressure, 0.5 for density, 0.5 for bulk force, 0.3 for momentum, 0.4 for turbulent kinetic energy, 0.4 for turbulent dissipation rate, 0.5 for turbulent viscosity, and 0.5 for energy, while the temperature is specified as the inlet water temperature under given conditions.

After the pre-processing, the computer commenced iterative execution and proceeded to compare the simulation results with experimental data for verification of simulation accuracy. The simulated operational conditions are presented in tab. 2.

Table 2. Simulation conditions

Conditions	PV/T collector	Radiation [Wm^{-2}]	Inlet temperature [°C]	Mass rate [Lpm]	Air temperature [°C]	Material
1-4	Parallel micro-channel PV/T	1000	25	0.6, 1.1, 1.5, 1.8	22	Stainless steel
5	Parallel micro-channel PV/T	600	40	1.1	18.2	Stainless steel
6-9	Three-passes micro-channel PV/T	1000	25	0.6, 1.1, 1.5, 1.8	22	Stainless steel
10	Three-passes micro-channel PV/T	600	40	1.1	23.5	Stainless steel

Validation

To validate the reliability of the model, a comparison was made between the simulation results of two distinct micro-channel PV/T collectors and experimental data. Figure 7 illustrates the infrared thermography of the parallel micro-channel PV/T collector under an irra-

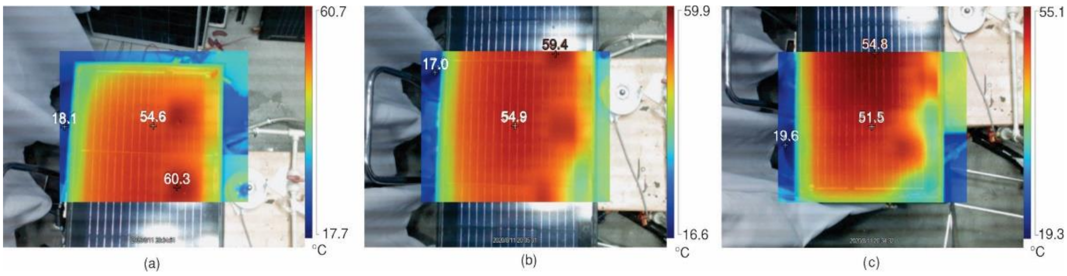

Figure 7. (a) Upper part of parallel micro-channel PV/T collector, (b) middle part of parallel micro-channel PV/T collector, and (c) lower part of parallel micro-channel PV/T collector

diance of 600 W/m^2, inlet water temperature of 40 °C, flow rate of 1.1 Lpm, and ambient temperature of 18.2 °C. The maximum temperature recorded for the PV cell was found to be 60.3 °C with an average temperature of 53.7 °C.

The simulation results, fig. 8, demonstrate the temperature distribution of a parallel micro-channel PV/T collector under operating conditions of irradiance at 600 W/m^2, inlet water temperature at 40 °C, and flow rate at 1.1 Lpm. The maximum temperature recorded for the PV/T system is 51.7 °C, with an average temperature of 51.0 °C. In comparison to experimental data, the maximum temperature is observed to be lower by 8.7 °C while the average temperature is lower by 2.7 °C. Furthermore, it can be observed that the temperature distribution within the PV cell exhibits regional variations, with lower temperatures near its perimeter compared to regions without direct contact with flow channels on both sides of the cell structure. The overall pattern of heat dissipation in the PV cell follows a corrugated trend spreading outwards from its center region; this simulated temperature distribution aligns more closely with experimental findings.

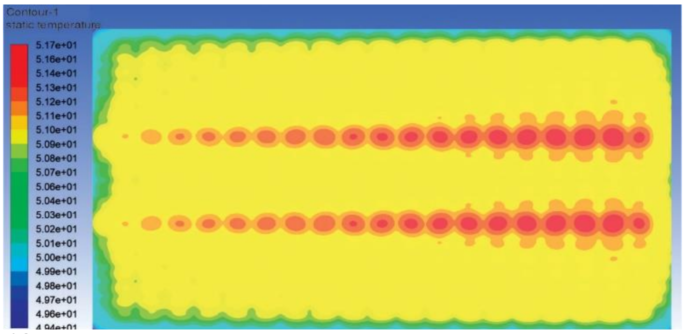

Figure 8. The temperature distribution of PV cell of parallel micro-channel PV/T

The infrared thermography of a three-passes micro-channel PV/T collector under the following working conditions: 600 W/m^2 irradiance, 40 °C inlet water temperature, 1.1 Lpm flow rate, and 23.5 °C ambient temperature is shown in fig. 9. The highest temperature recorded across the entire PV cell is 53.8 °C with an average temperature of 47.8 °C. It can be observed that the temperature distribution among the PV cells is more uniform, with lower temperatures on the right-hand side corresponding to the first pass of the runner and higher temperatures on the left-hand side corresponding to the third pass.

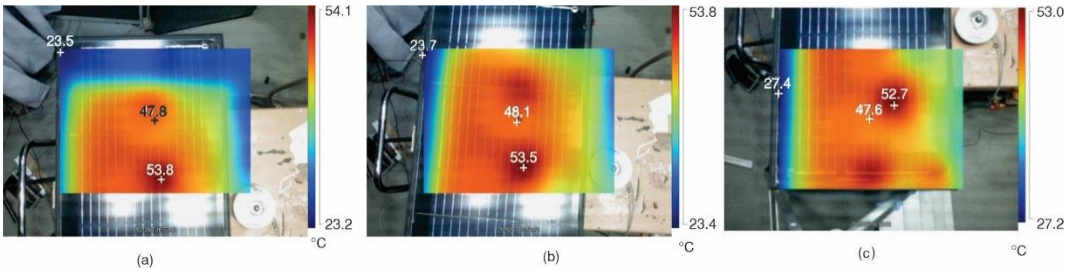

Figure 9. The infrared thermography of three-passes micro-channel PV/T collector; (a) upper part of three-passes micro-channel PV/T collector, (b) middle part of three-passes micro-channel PV/T collector, and (c) lower part of three-passes micro-channel PV/T collector

The temperature distribution of the PV cell under an irradiance of 600 W/m^2, inlet water temperature of 40 °C, and flow rate of 1.1 Lpm is depicted in fig. 10. The maximum temperature recorded for the PV cell reaches 51.3 °C, while the average temperature stands at 50.1 °C. Deviations between simulated results and experimental data are observed to be within a range of 2.5 °C for the maximum temperature and 2.3 °C for the average temperature respectively. Upon comparing these findings with experimental observations, it becomes evident that the simulated PV cell's thermal behavior closely aligns with real-world outcomes.

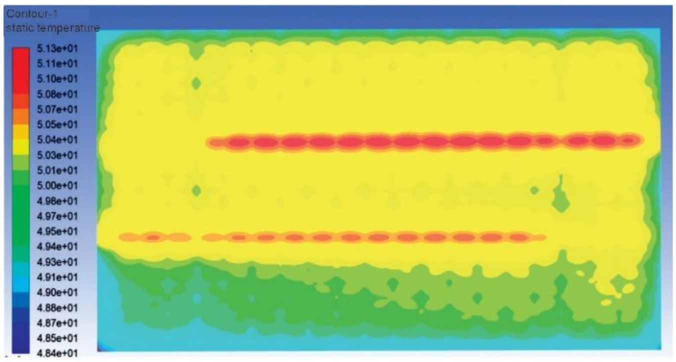

Figure 10. The temperature distribution of PV cell of three-passes micro-channel PV/T

Results and discussion

Parallel micro-channel PV/T

Analysis of certain conditions

The temperature distribution across the PV cell was investigated under specific conditions including an irradiance level of 1000 W/m^2, an inlet of 25 °C, and a flow rate of 1.1 Lpm as shown in fig. 11. Elevated temperatures are primarily concentrated in the rear half of the PV cell whereas fluid flow exerts a more significant influence on the front half leading to an increase in PV cell temperature along its longitudinal axis. The highest recorded temperature 56.9 °C with an average value measured at approximately 55.2 °C.

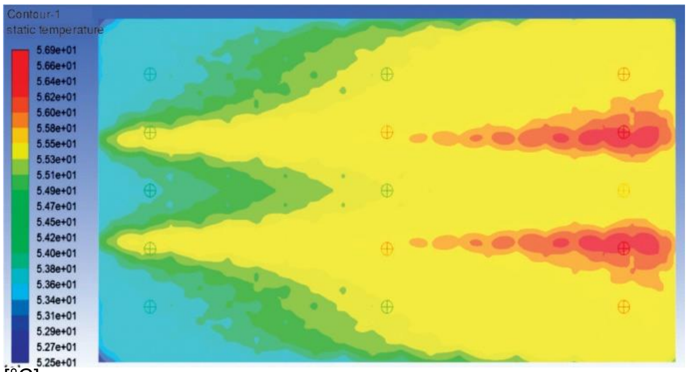

Figure 11. The temperature distribution of PV cell of parallel micro-channel PV/T

Figure 12 illustrates the temperature distribution of the fluid within the flow channel, with a maximum temperature of 32.3 °C and an average temperature of 27.6 °C. The fluid's temperature increases in the direction of flow, with higher temperatures on both sides of the flow channel and lower temperatures in its center. The outlet temperature is measured at 29.8 °C, while thermal efficiency reaches up to 43.6%.

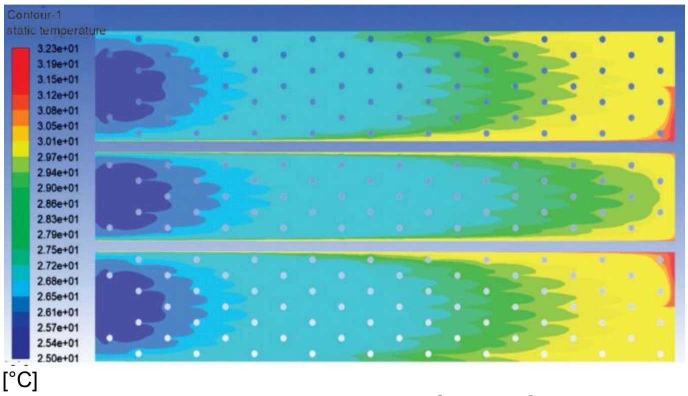

Figure 12. The temperature distribution of water of parallel micro-channel PV/T

The fluid velocity is depicted in fig. 13, exhibiting a maximum velocity of 0.174 and an average velocity of 0.035 m/s. Notably, the fluid velocity demonstrates variation across different flow channels, with higher velocities observed in the central channel and lower velocities in the left and right channels. The point of confluence between the header pipe and micro-channel represents the location of maximum fluid velocity.

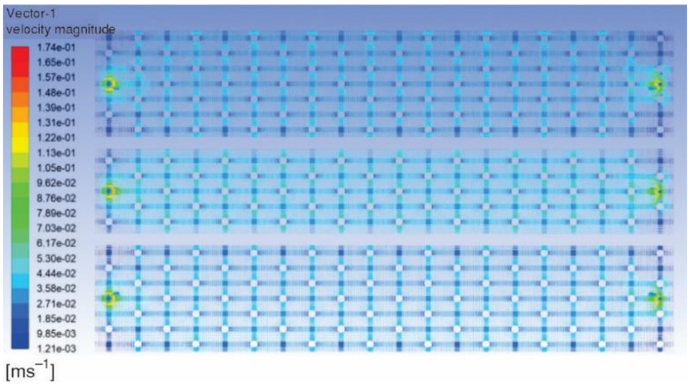

Figure 13. The velocity of fluid of parallel micro-channel PV/T

The pressure distribution of the fluid is illustrated in fig. 14, within the central flow channel and lower pressures in the adjacent channels. Furthermore, there is a gradual decrease in fluid pressure along the direction of flow, resulting in a total pressure drop of 550.9 Pa.

The effect of different mass flow rate

The temperature of the PV cell under different flow conditions is illustrated in fig. 15. Increasing the flow rate leads to a reduction in the average temperature of the PV cell and enhances its temperature uniformity. It can be observed from the figure that when the flow rate increases from 0.6-1.8 Lpm, there is standard deviation from 1.69 to 0.62. At a flow rate of 1.8 Lpm, the average temperature of the PV cell reaches 53.0 °C.

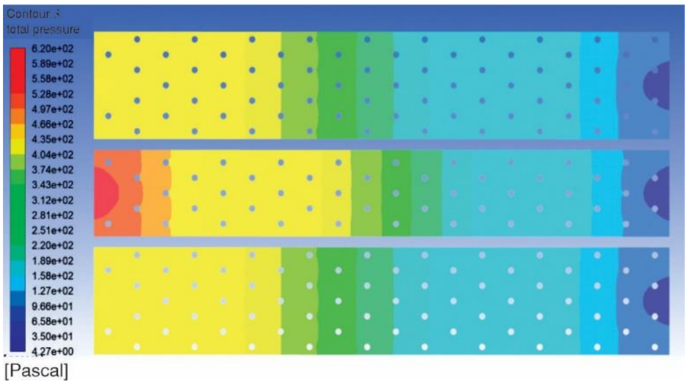

Figure 14. The fluid pressure clouds of parallel micro-channel PV/T

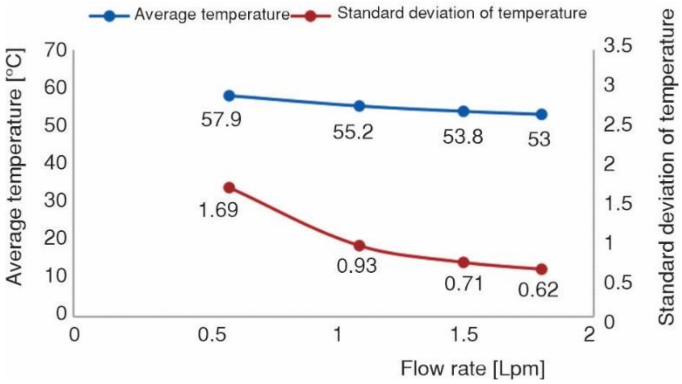

Figure 15. Average temperature of PV cell at different flow rates of parallel micro-channel PV/T

The pressure drops and maximum fluid velocity of parallel micro-channel PV/T under different flow conditions are illustrated in fig. 16. The impact increasing the flow rate on both pressures drops and maximum velocity is negligible at low flow rates, while they exhibit a more pronounced increase as the flow rate rises. The pressure drop at a flow rate of 1.8 Lpm is measured to be 939.2 Pa, while the corresponding maximum velocity is determined as 0.28 m/s.

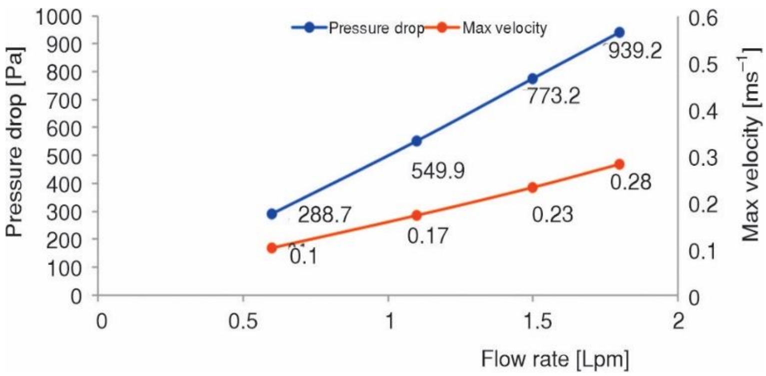

Figure 16. The pressure drops and max fluid velocity at different flow rates of parallel micro-channel PV/T

Analysis of working conditions at different ambient temperatures

Alter the wall surface to enhance convective heat transfer between the boundary conditions and the external environment. Figure 17 illustrates the thermal performance of the flat ambient temperatures. At an ambient temperature of 5 °C, the fluid's outlet water temperature reaches 25.8 °C with a corresponding thermal efficiency of 7.2%. Compared to typical operating conditions, there is a decrease in outlet water temperature by 4 °C and a reduction in thermal efficiency by 36.4%. These changes solely pertain to alterations in the temperature field. Consequently, minimizing heat loss during winter working conditions remains an imperative challenge for any PV/T device.

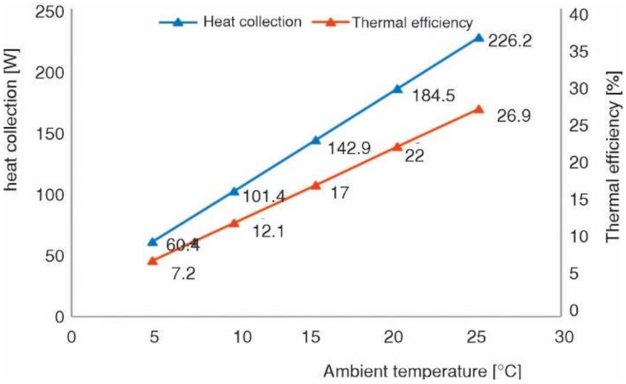

Figure 17. Heat collection and thermal efficiency at different ambient temperatures

Three-passes micro-channel PV/T

Analysis of typical working conditions

The temperature distribution of the PV cell under operating conditions with an irradiance of 1000 W/m^2, an inlet water temperature of 25 °C, and a flow rate of 1.1 Lpm is depicted in fig. 18. It reveals a maximum temperature of 53.7 °C and an average temperature of 50.1 °C.

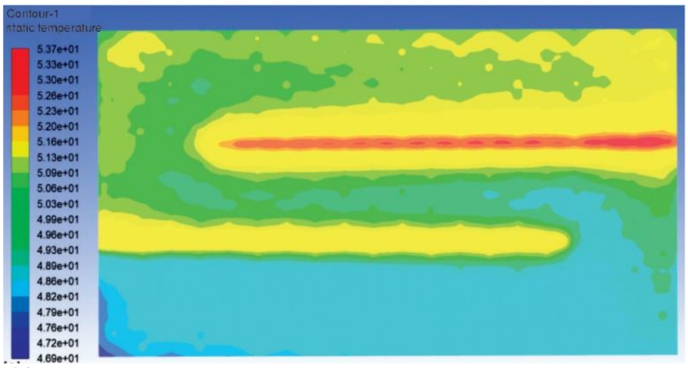

Figure 18. The temperature distribution of PV cell of three-passes micro-channel PV/T

The temperature distribution of the fluid in the flow channel is illustrated in fig. 19. The temperature gradient along the flow direction exhibits an increasing trend. Furthermore, at the end of the flow channel, both sides exhibit slightly higher temperatures compared to the middle region after two passes. The maximum temperature recorded within the entire flow channel reaches 37.4 °C, while the average temperature remains at 28.0 °C.

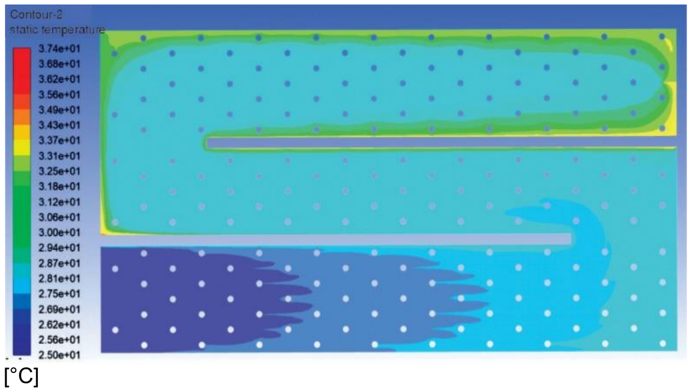

Figure 19. The temperature distribution of water of three-passes micro-channel PV/T

The fluid velocity is depicted in fig. 20, where it can be observed that the fluid diverges towards both the left and right sides as it approaches the orifice. Consequently, the velocity directly in front of and behind the orifice is reduced, while it increases on either side. The maximum velocity recorded is 0.48 m/s, with an average fluid velocity of 0.09 m/s.

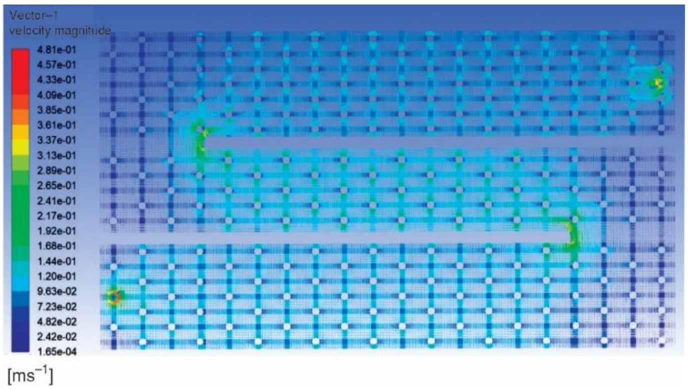

Figure 20. The velocity of fluid of three-passes micro-channel PV/T

The pressure cloud diagram of the fluid under a flow rate of 1.1 Lpm is presented in fig. 21. It can be observed that the fluid pressure gradually decreases along the direction of flow, while maintaining a relatively balanced pressure distribution on both sides of the channel. At the corner where the flow direction changes, there is a lower pressure in the outer fluid compared to the inner fluid, followed by restoration of balance. Overall, a pressure drop of 4486 Pa is observed across the entire three-passes micro-channel PV/T system.

The effect of different mass flow rate

The temperature of the PV cell under different flow conditions is illustrated in fig. 22. As the flow rate increases, there is a decrease in the average temperature of the PV cell, thereby

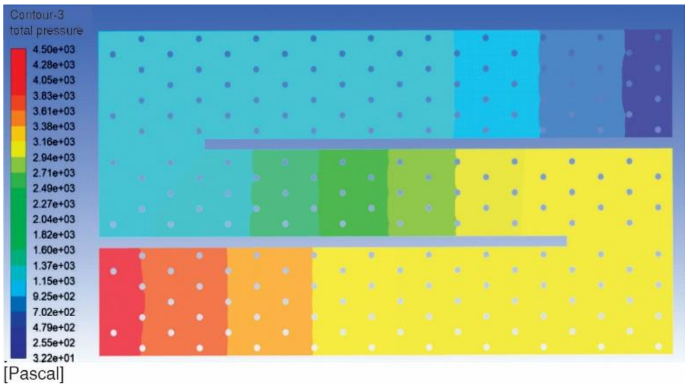

Figure 21. The fluid pressure clouds of three-passes micro-channel PV/T

enhancing the uniformity of its temperature distribution. Furthermore, with a continuous increase in flow rate, it can be observed that the standard deviation of PV panel temperature decreases from 2.18 to 1.05, indicating a more uniform distribution of temperatures across PV cells. Notably, when the flow rate was set at 1.8 Lpm, the average temperature of the PV cell reached 48.0 °C.

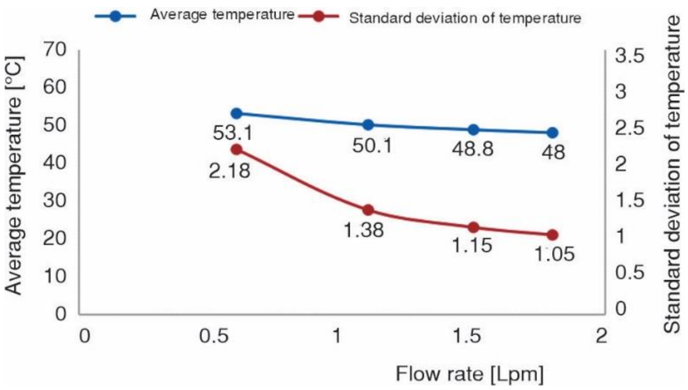

Figure 22. Average temperature of PV cell at different flow rates of three-passes micro-channel PV/T

The pressure drops and maximum fluid velocity of a three-passes micro-channel PV/T under different conditions were determined, and the corresponding results are presented in fig. 23. Increasing the flow rate at low levels has negligible impact on both pressure loss and maximum velocity. However, as the flow rate increases, there is an accelerated decrease in pressure along with an increase in maximum velocity. At a flow rate of 1.8 Lpm, the pressure drop was measured to be 7740.4 Pa, while the maximum speed reached 0.77 m/s.

Analysis of working conditions at different ambient temperatures

Modify the wall surface to enhance convective heat transfer with the external environment in the boundary conditions. Figure 24 illustrates the thermal performance of the three-passes PV/T system under varying ambient temperatures. The operational parameters include an irradiance of 1000 W/m^2, inlet water temperature of 25 °C, and flow rate of 1.1 Lpm. At an ambient temperature of 5 °C, the fluid's outlet water temperature reaches 26 °C with a thermal efficiency of 9.6%. Compared to typical operating conditions, there is a decrease in outlet water temperature by 4 °C and a reduction in thermal efficiency by 38.6%. As outdoor temperatures continue to rise, there is an increase in heat collection efficiency.

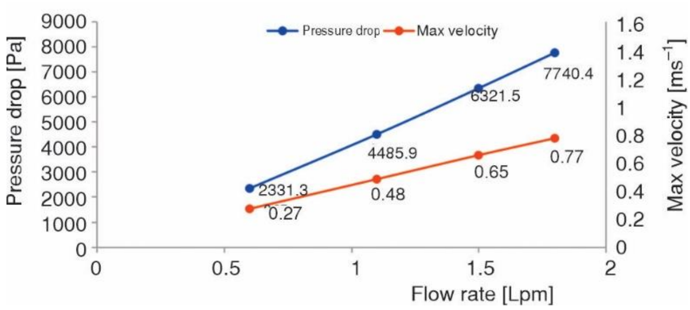

Figure 23. The pressure drops and maximum fluid velocity at different flow rates of three-passes micro-channel PV/T

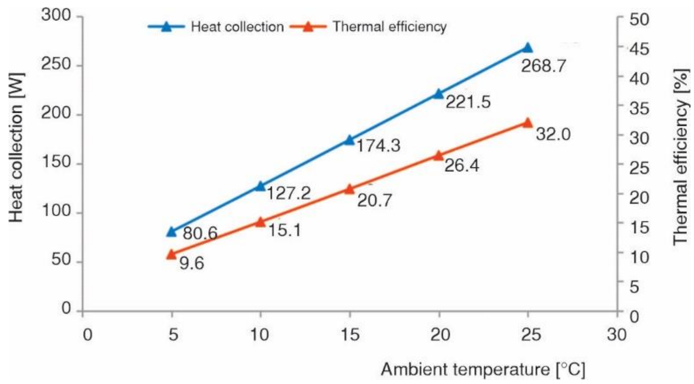

Figure 24. Heat collection and thermal efficiency at different ambient temperatures of three-passes micro-channel PV/T

Conclusions

By comparing the temperature distribution and uniformity of two types of micro-channel PV/T collectors at varying flow rates, evaluating the pressure drop characteristics and maximum achievable flow rate, as well as assessing the heat collection efficiency in different environmental conditions, several key findings can be deduced.

- The heat collection performance of the parallel micro-channel PV/T is slightly inferior to that of the three-passes micro-channel PV/T, exhibiting a 5.1% decrease at 25 °C. In winter operating conditions, both PV/T systems experience significant reductions in heat collection and efficiency. The three-passes PV/T system demonstrates a decline of 70% in heat collection and a decrease of 22 efficiency compared to summer conditions. Similarly, the parallel PV/T system experiences a reduction of 73% in heat collection efficiency and a decrease of 19.7% compared to summer.
- The parallel micro-channel PV/T exhibits a distinct advantage in terms of pressure drops. Under specific conditions, the pressure drops of the three-passes micro-channel are approximately 3935 Pa higher compared to those of the parallel micro-channel PV/T. Furthermore, an increase in flow rate from 0.6 Lpm to 1.8 Lpm results in a corresponding increase in pressure drops for both the current collector: by 650.5 Pa for the parallel micro-channel PV/T and by 5409.1 Pa for the three-passes micro-channel PV/T.

- The temperature uniformity of parallel micro-channel PV/T is superior to that of three-passes micro-channel PV/T. Under specific conditions, the temperature standard deviation of parallel micro-channel PV/T is reduced by 0.45 compared to three-return micro-channel PV/T, while the average temperature increases by 5 °C. Increasing the fluid flow rate leads to a decrease in PV cell temperature.

Follow-up research direction

In this experimental simulation, the primary focus lies in investigating the heat collection performance of PV/T collectors with varying micro-channels. Subsequent simulations will be conducted to assess the power generation performance of PV/T and identify disparities among different micro-channel collectors. Furthermore, by integrating the average temperature of the collector with the heat collection and power generation efficiency of PV/T plates, optimal working temperatures for diverse collectors can be determined.

Acknowledgment

The research is supported by the National Natural Science Foundation of China (No. 71974129).

References

[1] Wolf, M., Performance Analyses of Combined Heating and PV Power Systems for Residences, *Energy Conversion.*, *16* (1976), 1-2, pp. 79-90
[2] Baljit, S. S. S., *et al.*, Review of Building Integrated Applications of PV and Solar Thermal Systems, *Journal of Cleaner Production*, *137* (2016), Nov., pp. 677-689
[3] Yang, T., Athienitis, A. K., A Review of Research and Developments of Building-Integrated PV/Thermal (BIPV/T) Systems, *Renewable and Sustainable Energy Reviews*, *66* (2016), Dec., pp. 886-912
[4] Debbarma, M., *et al.*, Thermal Modeling, Exergy Analysis, Performance of BIPV and BIPVT: A Review, *Renewable and Sustainable Energy Reviews*, *73* (2017), June, pp. 1276-1288
[5] Shukla, A. K., *et al.*, Recent Advancement in BIPV Product Technologies: A Review, *Energy Build*, *140* (2017), Apr., pp. 188-195
[6] Wei, H., *et al.*, Hybrid PV and Thermal Solar-Collector Designed for Natural Circulation of Water, *Applied Energy*, *83* (2006), 3, pp. 199-210
[7] Yandri, E., Modeling Joule Heating Effect on Thermal Efficiency of PV Thermal Collectors with Operation Mode Factor, *Applied. Science*, *12* (2022), 2, 742
[8] Zhou, J., *et al.*, Numerical Simulation and Experimental Validation of a Micro-Channel PV/T Modules Based Direct-Expansion Solar Heat Pump System, *Renewable Energy*, *145* (2020), Jan., pp. 1992-2004
[9] Atazaz, H., *et al.*, An Experimental and Numerical Study on the Impact of Various Parameters in Improving the Heat Transfer Performance Characteristics of a Water Based PV Thermal System, *Renewable Energy*, *202* (2023), Jan., pp. 499-512
[10] Tahmasbi, M., *et al.*, Thermal and Electrical Efficiencies Enhancement of a Solar PV-Thermal/Air System (PV/T/Air) Using Metal Foams, *J. of the Taiwan Institute of Chem. Eng.*, *124* (2021), July, pp. 276-289
[11] Satpute, J., Rajan, J., Analysis of Energy, Exergy, Environmental, and Economics (4e) on PV-Thermal Collector System. *Thermal Science*, *26* (2022), 5B, pp. 4233-4247
[12] Deng, Y., *et al.*, Experimental Study of the Thermal Performance for the Novel Flat Plate Solar Water Heater with Micro Heat Pipe Array Absorber, *Energy Procedia*, *70* (2015), May, pp. 41-48
[13] Hesham, I. E., *et al.*, Concentrator PV Thermal Management Using a New Design of Double-Layer Micro-Channel Heat Sink, *Solar Energy*, *220* (2021), May, pp. 552-570

Paper submitted: May 22, 2023
Paper revised: July 15, 2023
Paper accepted: October 3, 2023